AN ADAPTIVE PD CONTROLLER WITH ODD-HARMONIC REPETITIVE COMPENSATION FOR UPS APPLICATIONS

Márcio Stefanello and Hilton Abílio Gründling
Universidade Federal de Santa Maria - UFSM
Grupo de Eletrônica de Potência e Controle - GEPOC
Av. Roraima S/N, Camobi, 97105-900, Santa Maria, RS, Brazil
E-mail: marciost@ieee.org, ghilton@ctlab.ufsm.br

***Abstract*— This paper proposes the application of the Model Reference Adaptive Controller (MRAC) concepts to the continuous adaptation framework of a discrete Proportional Derivative (PD) control law. In order to compensate the nonlinear load disturbances in UPS applications, a modified Repetitive (RP) plug-in action is added. Besides the nonlinear load-effect compensation, the proposed MRAC-PD controller allows the tracking of the plant output with respect to a reference model output. In order to demonstrate the overall control feasibility, the algorithm was implemented in a TMS320F2812 DSP controller and experimental results for a 6kVA three-phase UPS system are presented to support the theoretical developments.**

***Keywords* – MRAC controller, modified Repetitive action, odd-harmonic compensation.**

I. INTRODUCTION

Uninterruptible Power Systems (UPS) have been extensively used as a backup system for single and three-phase critical loads. The UPS requirements are defined by standards such as the IEC62040-3 [1], which imposes limits on the THD (Total Harmonic Distortion) of the output voltages and classifies the UPS according to its performance. Thus, researches on UPS relates to its topology and control strategies to reach such requirements. In its majority, typical loads are comprised by diode bridges with capacitive filter, and control strategies based on RP plug-in controllers have been considered to mitigate the resultant undesired distortions on the voltage waveform [2], [3]. The plug-in RP controllers are embedded with a main controller in order to provide certain stability margins. Nevertheless, a few researches on RP schemes are concerned with this controller. In [3], [4], the use of an adaptive scheme was proposed to tune the gain of the RP controller. The system was based on a robust model reference adaptive control (RMRAC) with a conventional RP controller [5]. In the same lines, this paper develops a direct MRAC-PD compensator with a modified RP controller. The adaptive design is so that, parametric deviations from the nominal plant are compensated and the output of the plant tracks a predefined reference model output. Such scheme provides a direct adaptive control law and a Gradient algorithm can used either in a continuous adaptation approach or as an aid design tool. The RP action is based in works of [6]–[8]. These approaches differ from the conventional RP schemes [2]–[5], [9] as the transfer function of the controller can be adjusted in order to comprise only selected harmonics components for compensation. Thus, this approach presents a reduced number of states improving the transient response. Moreover, the undesired plant and controller dynamics cancelation can be avoided [8]. This problem arises, for example, when an output transformer is connected at the UPS output because the plant model appears with a zero $z = 1$. Once from the internal model principle any pole/zero cancelation must be prevented, the use of a conventional RP approach violates this statement and the controller presented in this paper is a candidate approach. Besides, the algorithm can be improved in order to demand less use of memory in an experimental implementation. This is achieved by using a multi–rate framework where the RP controller is sampled in a multiple rate lower than the MRAC-PD controller.

In this paper, the compensation was limited to the odd-harmonic components and the pole in the origin was suppressed. In the following sections, the adaptive algorithm is described. After, the modified RP scheme is shown and finally, the overall system and the design parameters are given. Some simulation and experimental results are presented to verify the system feasibility.

II. MRAC-PD CONTROLLER

The overall control approach consists of two control loops, comprising the MRAC-PD (see Figure 1) and the RP plug-in controller.

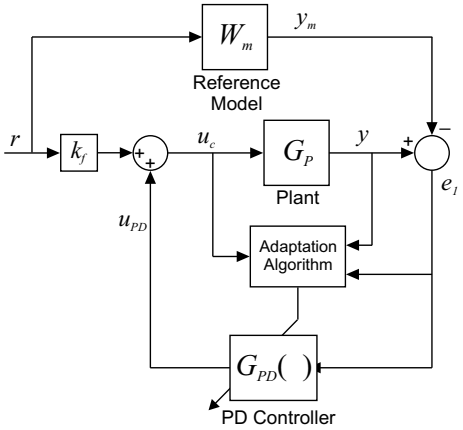

Fig. 1: Block diagram of MRAC-PD system

A. Plant and Reference Model Assumptions

Let us consider the following SISO plant in terms of the discrete operator z

$$\frac{y(z)}{u_c(z)} = G_p(z) = k_p \frac{Z_0(z)}{R_0(z)}. \quad (1)$$

Where $G_p(z)$ is a strictly proper transfer function. Lets too introduce a stable transfer function for the reference model.

$$\frac{y_m(z)}{r(z)} = W_m(z) = k_m \frac{1}{D_m(z)}. \quad (2)$$

The assumptions for (1) and (2) (see [10]) are stated bellow:

A1: $Z_0(z)$ is a monic Hurwitz polynomial with degree $m \leq n-1$;
A2: $R_0(z)$ is a monic polynomial with degree n;
A3: The sign of k_p is known;
A4: m and n are known;
A5: $D_m(z)$ is a monic Hurwitz polynomial with degree $n^* = n - m$;

The objective of a MRAC based controller is, given a reference model with output y_m, design an adaptive controller so that the closed–loop plant is stable and the plant output y tracks y_m as closely as possible.

B. MRAC-PD Control Law and Error Equation

A discrete PD compensator can be expressed in terms of the transfer function

$$\frac{u_{PD}(z)}{e_1(z)} = G_{PD}(z) = \theta_P + \theta_D \left(1 - z^{-1}\right). \quad (3)$$

In the difference equation form, follows from (3) that

$$u_{PD}(k) = \theta_1(k) e_1(k) + \theta_2(k) e_1(k-1),$$

where $\theta_1 = \theta_P + \theta_D$, $\theta_2 = -\theta_D$ with θ_P, θ_D defined as the discrete–time proportional and derivative gains.

From Figure 1, the control law u_c is given by

$$u_c(k) = k_f r(k) + \theta_1(k) e_1(k) + \theta_2(k) e_1(k-1). \quad (4)$$

where k_f is a positive constant and r is an uniform bounded signal.

Assuming

$$\theta(k)^T \triangleq \begin{bmatrix} \theta_1(k) & \theta_2(k) \end{bmatrix} \text{ and}$$
$$\omega(k)^T \triangleq \begin{bmatrix} e_1(k) & e_1(k-1) \end{bmatrix},$$

and from (4), the resultant control law is given by

$$u_c(k) = k_f r(k) + \omega(k)^T \theta(k). \quad (5)$$

In order to obtain the augmented error, we next define the tracking error $e_1 = y - y_m$ and the parametric error vector $\phi = \theta^T - \theta^{*T}$. Subtracting the term $\theta^{*T}\omega$ in both sides of (5) results in

$$u_c(k) - \theta^{*T}(k)\omega(k) = k_f r(k) + \phi^T(k)\omega(k). \quad (6)$$

Considering the objective of the reference model approach stated in the previous section and from (1) and (2), follows that

$$y(k) = G_p(z) u_c(k) = y_m(k) = W_m(z) r(k).$$

In such ideal case, the parametric error vector is $\phi = \begin{bmatrix} 0 & 0 \end{bmatrix}^T$ and with this assumption follows from (6) that

$$k_f r(k) = u_c(k) - \theta^{*T}(k)\omega(k). \quad (7)$$

The substitution of $r(k) = W_m(z)^{-1} y(k)$ in (7) gives

$$y(k) = k_f^{-1} W_m [u_c(k) - \theta^{*T}(k)\omega(k)].$$

In the above equation, the term inside the brackets can be replaced in according with (6). The plant output can now be expressed as

$$y(k) = k_f^{-1} W_m [k_f r(k) \phi^T(k)\omega(k)],$$

and the tracking error e_1 is given by

$$e_1(k) = y(k) - y_m(k) = k_f^{-1} W_m \phi^T(k)\omega(k). \quad (8)$$

We now define an augmented error equation using the following relation

$$W_m \phi^T \omega - \phi^T W_m \omega = -\theta^T W_m \omega + W_m \theta^T \omega.$$

By replacing the term $W_m(z)\phi^T\omega$ in (8), the augmented error is

$$\varepsilon(k) = e_1(k) + \theta(k)^T \xi(k) - W_m(z) v(k) = \phi(k)^T \xi(k), \quad (9)$$

where $\xi = W_m(z) I \omega$ and $v = \theta^T \omega$.

C. Parameter Adaptation Algorithm

Consider the following adaptive algorithm

$$\theta(k+1) = (I - \sigma T_s P)\,\theta(k) - T_s P \frac{\xi(k)\varepsilon(k)}{1 + m(k)^2}, \quad (10)$$

where $P = P^T > 0$.

The normalization signal is given by

$$m(k+1) = (1 - T_s \delta_0)\, m(k) + \ldots$$
$$T_s \delta_1 \left(|u(k)| + |y(k)| + 1\right),$$

with $m(0) \geq \frac{\delta_1}{\delta_0}$, $\delta_1 \geq 1$ and δ_0 is a positive constant. The terms ε and ξ were defined in the previous section.

The *σ-modification* used in (10) is given by

$$\sigma = \begin{cases} 0 & \text{if } \|\theta\| < M_0 \\ \sigma_0 \left(\frac{\|\theta\|}{M_0} - 1\right) & \text{if } M_0 \leq \|\theta\| < 2M_0 \\ \sigma_0 & \text{if } \|\theta\| > 2M_0 \end{cases}$$

where M_0 is an upper bound for $\|\theta^*\|$ and σ_0 has a positive value.

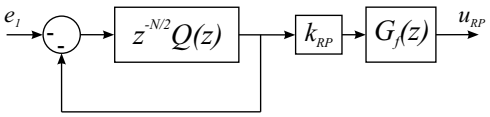

Fig. 2: Negative feedback loop with odd-harmonic generation capability

III. Modified RP Controller

From the internal model principle, the plant output can track a class of reference commands if the generator for the references is included in a stable closed–loop system. In this paper, a discrete–time module for generation of odd–harmonic commands is used as in [7]. The realization of such reference generator can be implemented by the use of the negative feedback structure depicted in Figure 2. The resultant transfer function is given by

$$\frac{u_{RP}(z_m)}{e_1(z_m)} = G_{RP}(z_m) = \frac{N(z_m)}{\phi(z_m)}. \qquad (11)$$

The use of the new discrete–time operator z_m is related to the particular sample time T_m of the RP controller, which can differ from the basis sampling–time T_s of the MRAC–PD controller. This multi–rate sampling scheme is depicted in Figure 3. The method consists on to sample the RP controller at each n_s samples of the MRAC–PD control law. The sampling times are properly chosen so that $T_m = n_s T_s$ shall lead to an even integer value of N samples of (11) over one fundamental period $T_1 = 1/f_1$, where f_1 is the fundamental frequency of the output waveform.

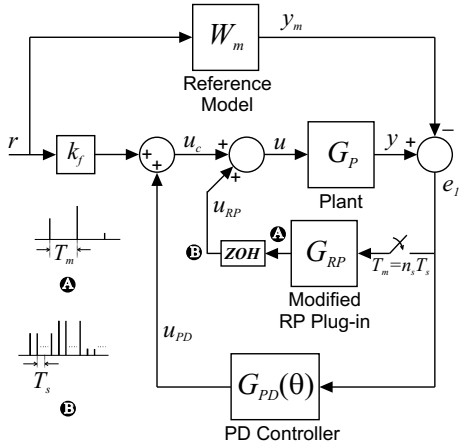

Fig. 3: Block diagram of the overall system in the proposed multi–rate approach

In (11), the polynomial $\phi(z_m)$ comprises all the frequencies to be rejected and $N_m(z_m)$ depends on the transfer function $G_f(z_m)$ and the gain k_{RP}. In this paper, the transfer function G_{RP} is given by

$$G_{RP}(z_m) = k_{RP}\frac{z_m^d}{z_m^{N/2} + Q(z_m, z_m^{-1})}, \qquad (12)$$

To enhance the robustness, it is usual the insertion of a FIR low–pas filter $Q(z_m, z_m^{-1})$ such that $\left\|Q(z_m, z_m^{-1})\right\| \leqslant 1$, with zero phase shift at the fundamental frequency f_1 of the reference r. The parameter d is used to compensate the phase lead introduced by the plant.

The pole–zero map for the RP controller in the cases where the low-pass filter is made $Q = 1$ and $Q(z_m, z_m^{-1}) = 0.25z_m^{-1} + 0.5 + 0.25z_m$ is shown in Figure 4. In the present example, the discrete–time functions generators were sampled at $T_m = 1/1920Hz$. Hence, a total number of $N = 32$ samples were accomplished over one fundamental period $f_1 = 60Hz$. Furthermore, the choice of the new frequency $f_m = f_s/N$ decreases the number of poles in the closed–loop transfer function, improving the transient time response.

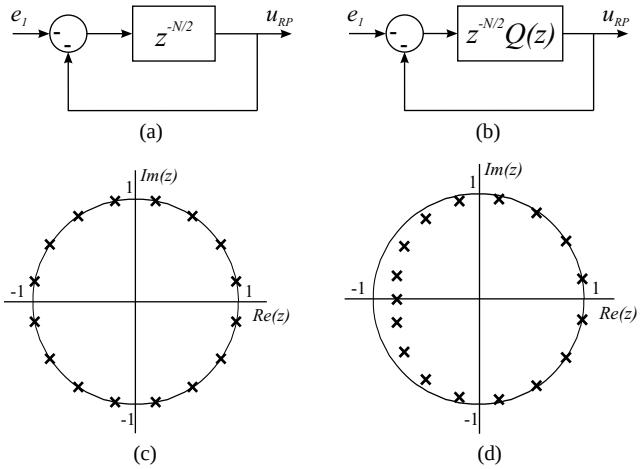

Fig. 4: Pole–zero maps (c) and (d) for the blocks (a) and (b) respectively

As seen from the pole–zero map in Figure 4d, the selection of the FIR filter $Q(z_m, z_m^{-1})$ brings to a dumping on the poles, which are now more closely inside the unit circle edge. Thus, this approach increases the robustness but may compromises the compensation performance at those frequencies, if compared to the case were $Q = 1$ (see Figure 4b).

IV. Results and Discussions

The MRAC–PD controller embedded with the modified RP controller was simulated for the three–phase UPS system of Figure 5.

For all results, the reference model was

$$W_m(z) = \frac{0.017z^{-1} + 0.016z^{-2}}{1 - 1.807z^{-1} + 0.841z^{-2}}.$$

A. Simulation Results

The simulated system parameters were: $L_0 = 400mH$, $C_0 = 130\mu F$, $R_s = 0.25\Omega$, $R_1 = 10\Omega$ and $C_1 = 11300\mu F$. The values R_1, R_s, C of the nonlinear load were obtained in compliance with the IEC62040-3 standard. Which has been considered in the majority of UPS related papers, since it defines tight performance limits and can be considered as a

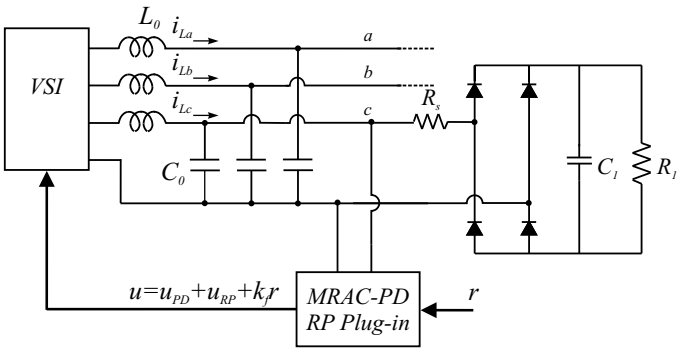

Fig. 5: LC filter and rectified load

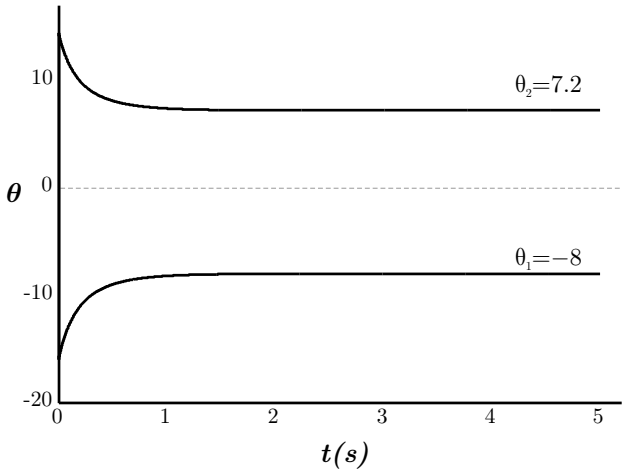

Fig. 7: Parametric convergence of the MRAC-PD compensator

reference for comparison between different UPS equipments by defining a common load test.

For the simulation results, the MRAC–PD related parameters were initialized with $k_f = 1$, $\theta_0 = \begin{bmatrix} -16 & 14 \end{bmatrix}^T$, $P = 10I_{2\times 2}$, $\sigma_0 = 0.3$, $M_0 = 10.7$, $\delta_0 = 0.5$ and $\delta_1 = 1$ with the sampling frequency $f_s = 19200Hz$. For the RP plug–in controller, the gains are $k_{RP} = 1.014$, $N = 64$, $d = 2$ and $n_s = 5$. The FIR filter used in (12) was chosen as $Q(z_m) = 0.25z_m^{-1} + 0.5 + 0.25z_m$ and the resultant sampling frequency of the RP servo system is $f_m = 3840Hz(f_s/n_s)$.

The tracking capability of the plant output y toward the reference model output y_m under a nonlinear load is shown in Figure 6 for a $60Hz/127Vrms$ waveform. Figure 7 shows the evolution of the parameter vector θ (5). As $\theta_1 = \theta_P + \theta_D$ and $\theta_2 = -\theta_D$, the discrete proportional and integral PD gains are $\theta_P = -0.8$ and $\theta_D = -7.2$.

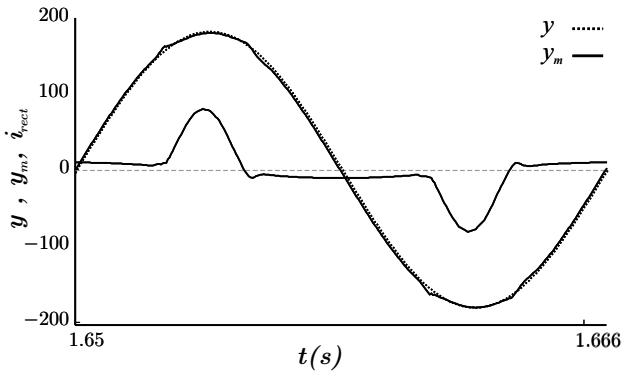

Fig. 6: Reference Model output y_m, corresponding phase voltage y and current, driven by a single-phase rectified load

B. Experimental Results

An equivalent 6kVA prototype using IGBT switches was implemented and tested. Due to practical reasons, the L_0C_0 filter and load parameters are the same of the simulated example with exception of the load filter capacitor $C_1 = 9400\mu F$ and the output voltage was set to $110V_{rms}$. In this case, the initial MRAC-PD parameters are $\theta_0 = \begin{bmatrix} -4 & 3.6 \end{bmatrix}^T$, $M_0 = 2$ and the filter is $Q(z_m) = 0.025z_m^{-1} + 0.95 + 0.025z_m$ in order to increase the performance of the RP controller. All the rest of parameters were kept the same.

To verify the transient behavior of the system with the adaptive scheme, a step of 50% on the reference value was implemented. As seen in Figure 8, the plant output y tracks the reference signal y_m. It is important to point out that the mismatching between the waveforms are due to the high nonlinear behavior of the loads.

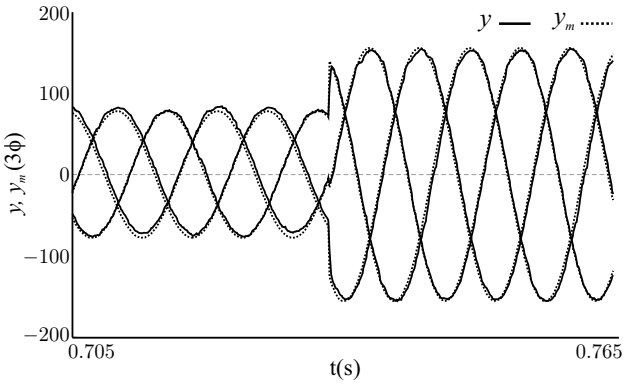

Fig. 8: Reference step of 50% and tracking behavior

Next, Figure 9 shows the parametric convergence for the previous experiment. The final values of the parameter vector leads to proportional and derivative discrete gains $\theta_P = -1.16$ and $\theta_D = -1.33$.

A load transition experiment was realized in order to evaluate the closed–loop tracking error limit. In Figure 10 the plant output and the resulting tracking error e_1 are shown. In spite of the high error in the transitions, the steady–state values decreases to less than 6%. The fundamental amplitude waveform is $125V$. In the Figure 11a and 11b the steady–state output waveforms are shown for the conditions of nominal nonlinear load and no–load, respectively. In all simulation and experimental results the THD in steady–state conditions not exceeded the range of 1.5%.

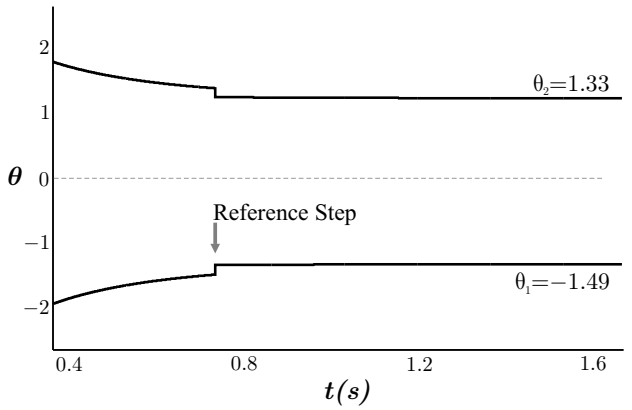

Fig. 9: Parametric convergence for the experiment of Figure 8

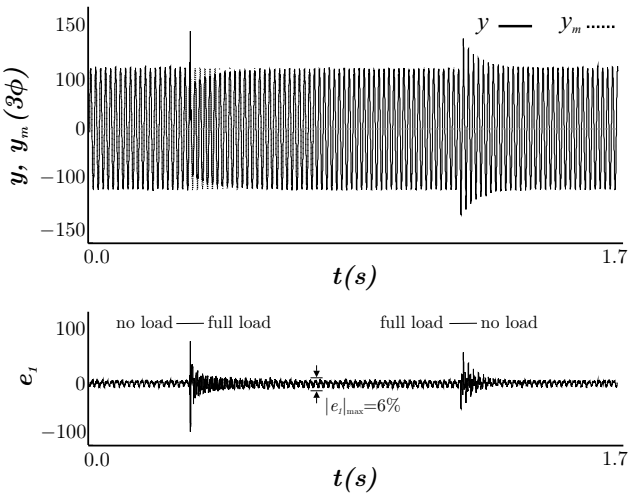

Fig. 10: Output phase voltage and rectified load current

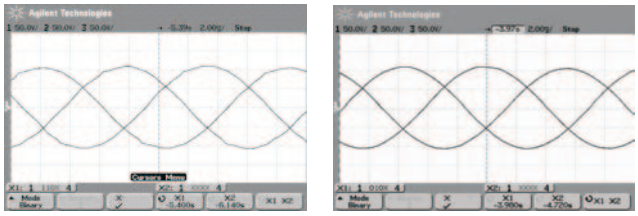

(a) (b)

Fig. 11: Output voltage waveforms for nonlinear load (a) with THD=1.5% and no–load (b).

V. Conclusion

This paper proposes an adaptive approach embedded in a RP plug-in controller for odd-harmonic suppression in a multi-rate framework. The simulated and experimental results pointed out the effectiveness of the adaptive algorithm once the norm of the parameters converges to a previous known control parameter M_0 and do not diverges. Moreover, by reducing the sampling rate of the RP action, it is possible to improve the stability margins as well as the transient response of the overall system. Experimental results from a 6kVA three-phase inverter demonstrated the good performance of the proposed approach.

Acknowledgment

The authors would like to thanks CAPES, CNPQ and FAPERGS for financial support.

References

[1] *Uninterruptible Power Systems (UPS)-Part 3: Method of Specifying the Performance and Test Requirements*, International Electrotechnical Commission, International Standard IEC 62 040-3.

[2] T. Haneyoshi, A. Kawamura, and R. G. Hoft, "Waveform compensation of pwm inverter with cyclic fluctuating loads," *IEEE Transactions on Industry Applications*, vol. 24, no. 4, pp. 582–589, Jul/Aug 1988.

[3] É. G. Carati, J. R. Pinheiro, and H. A. Gründling, "A robust model reference adaptive controller for ups applications," in *Proc. of 23rd IECON'97*, vol. 2. New Orleans, LA, USA: Industrial Electronics Society, Nov 1997, pp. 901–905.

[4] ——, "Analysis and implementation of a modified robust model reference adaptive control with repetitive controller for ups applications," in *Proc. of 24rd IECON'98*, vol. 1. Aachen, Germany: Industrial Electronics Society, Aug 1998, pp. 391–395.

[5] C. Rech, H. Pinheiro, H. A. Gründling, H. L. Hey, and J. R. Pinheiro, "Comparison of digital control techniques with repetitve integral action for low cost pwm inverters," *IEEE Transactions on Power Electronics*, vol. 18, no. 1, pp. 401–410, Jan 2003.

[6] X. Kong, J. Wang, L. Peng, Y. Kang, and J. Cheng, "The control technique of three-phase voltage-source inverter output waveform based on internal model theory," in *Proc. of 29th IECON'03*, vol. 1. Roanoke, Virginia, USA: Industrial Electronics Society, Nov 2003, pp. 788–793.

[7] R. Costa-Castelló, R. Griño, and E. Fossas, "Odd-harmonic digital repetitive control of a single-phase current active filter," *IEEE Transactions on Power Electronics*, vol. 19, no. 4, pp. 1060–1068, Jul 2004.

[8] F. Botterón and H. Pinheiro, "Discrete-time internal model controller for three-phase pwm inverters with insulator transformer," *IEE Proc. on Power Electronics Applications*, vol. 153, no. 1, pp. 57–67, Jan 2006.

[9] K. Zhou and D. Wang, "Digital repetitive learning controller for three-phase cvcf pwm inverter," *IEEE Transactions on Industry Applications*, vol. 48, no. 4, pp. 820–830, Aug 2001.

[10] P. A. Ioannou and K. S. Tsakalis, "A robust direct adaptive controller," *IEEE Transactions on Automatic Control*, vol. AC-31, no. 11, pp. 1033–1043, Nov 1986.